Integrating Clinical Variables, Radiomics, and Tumor-derived Cell-Free DNA for Enhanced Prediction of Resectable Esophageal Adenocarcinoma Outcomes

Ende, Tom van den; Kuijper, Steven C.; Widaatalla, Yousif; Noortman, Wyanne A.; Woodruff, Henry C.; van der Pol, Ymke; Moldovan, Norbert; de Geus-Oei, Lioe Fee; van Laarhoven, Hanneke W.M.; More Authors

DOI
10.1016/j.ijrobp.2024.10.010

Publication date
2025

Document Version
Final published version

Published in
International Journal of Radiation Oncology Biology Physics

INTERNATIONAL JOURNAL OF
RADIATION ONCOLOGY • BIOLOGY • PHYSICS
www.redjournal.org

CLINICAL INVESTIGATION

Integrating Clinical Variables, Radiomics, and Tumor-derived Cell-Free DNA for Enhanced Prediction of Resectable Esophageal Adenocarcinoma Outcomes

Tom van den Ende, MD,[*,†] Steven C. Kuijper, MSc,[*,†] Yousif Widaatalla, MD,[‡] Wyanne A. Noortman, MSc,[§,‖] Floris H.P. van Velden, PhD,[§] Henry C. Woodruff, PhD,[‡,¶] Ymke van der Pol, MSc,[†,#] Norbert Moldovan, PhD,[†,#] D. Michiel Pegtel, PhD,[†,#] Sarah Derks, MD,[†,**,††] Maarten F. Bijlsma, PhD,[†,††,‡‡] Florent Mouliere, PhD,[†,#] Lioe-Fee de Geus-Oei, MD,[§,‖,§§] Philippe Lambin, MD,[‡,¶] and Hanneke W.M. van Laarhoven, MD[*,†]

[*]*Department of Medical Oncology, Amsterdam UMC, University of Amsterdam, Amsterdam, The Netherlands;* [†]*Cancer Center Amsterdam, Imaging and Biomarkers, Amsterdam, The Netherlands;* [‡]*The D-Lab, Department of Precision Medicine, GROW-School for Oncology and Reproduction, Maastricht University, Maastricht, The Netherlands;* [§]*Department of Radiology, Section of Nuclear Medicine, Leiden University Medical Center, Leiden, The Netherlands;* [‖]*TechMed Centre, University of Twente, Enschede, The Netherlands;* [¶]*Department of Radiology and Nuclear Medicine, Maastricht University Medical Center, Maastricht, The Netherlands;* [#]*Department of Pathology, Amsterdam UMC, Vrije Universiteit Amsterdam, Amsterdam, The Netherlands;* [**]*Department of Oncology, Amsterdam UMC, Vrije Universiteit Amsterdam, Amsterdam, The Netherlands;* [††]*Oncode Institute, Utrecht, The Netherlands;* [‡‡]*Laboratory for Experimental Oncology and Radiobiology, Center for Experimental and Molecular Medicine, Amsterdam UMC, University of Amsterdam, Amsterdam, The Netherlands; and* [§§]*Department of Radiation Science & Technology, Delft University of Technology, Delft., The Netherlands*

Received Mar 25, 2024; Accepted for publication Oct 6, 2024

Purpose: The value of integrating clinical variables, radiomics, and tumor-derived cell-free DNA (cfDNA) for the prediction of survival and response to chemoradiation of patients with resectable esophageal adenocarcinoma is not yet known. Our aim was to investigate if radiomics and cfDNA metrics combined with clinical variables can improve personalized predictions.

Corresponding author: Hanneke W.M. van Laarhoven, MD; E-mail: h.vanlaarhoven@amsterdamumc.nl

Tom van den Ende and Steven C. Kuijper made equal contributions to this study.

Disclosures: H.C.W. has minority shares with the company Radiomics SA and is coinventor on patents for radiomics. D.M.P. is founder and shareholder of ExBiome; has consulted for Takeda; and received grant funding from Takeda, Prediction Biosciences, and Gilead. M.F.B. received research funding from Celgene, Frame Therapeutics, and Lead Pharma; and has acted as a consultant for Servier and Olympus. F.M. has consulted for Roche Diagnostics, and is coinventor on patents for cell-free DNA analysis. P.L. within the submitted work, reports grants or sponsored research agreements with Radiomics SA & Convert Pharmaceuticals; received a presenter fee (in cash or in kind) and/or reimbursement of travel costs/consultancy fee (in cash or in kind) from Radiomics SA, BHV; minority shares in the company's Radiomics SA and Convert pharmaceuticals; coinventor of 2 issued patents with royalties on radiomics (PCT/NL2014/050248 and PCT/NL2014/050728), licensed to Radiomics SA; 3 nonpatented inventions (software) licensed to Theragnostic/DNAmito, Radiomics SA and 1 nonissued, nonlicensed patents on Deep Learning-Radiomics (N2024482, N2024889), and confirms that none of the above entities were involved in the preparation of this paper. H.W.M.v.L. reports as consultant for BMS, Daiichi, Dragonfly, Eli Lilly, MSD, Nordic Pharma, and Servier; research funding, and/or medication supply from Bayer, BMS, Celgene, Janssen, Incyte, Eli Lilly, MSD, Nordic Pharma, Philips, Roche, and Servier; speaker role for Astellas, Daiichy, and Novartis. The other authors report no conflicts of interest. N.M. and F.M. are supported by a Dutch Cancer Fund (KWF-12822). The PERFECT study was financially supported by Hoffmann-La Roche Ltd., Basel, Switzerland. Analysis of cell-free DNA of the neoadjuvant chemoradiation therapy cohort was made possible through a grant of the Maag Lever Darm Stichting (SK18-32). Funders had no role in the design of the study.

Data Sharing Statement: The data sets used and/or analyzed during this study will be shared upon request to the corresponding author.

Supplementary material associated with this article can be found, in the online version, at doi:10.1016/j.ijrobp.2024.10.010.

Int J Radiation Oncol Biol Phys, Vol. 121, No. 4, pp. 963–974, 2025

https://doi.org/10.1016/j.ijrobp.2024.10.010

Methods and Materials: A cohort of 111 patients with resectable esophageal adenocarcinoma from 2 centers treated with neoadjuvant chemoradiation therapy was used for exploratory retrospective analyses. Models combining the clinical variables of the SOURCE survival model with radiomic features and cfDNA were built using elastic net regression and internally validated using 5-fold cross-validation. Model performance for overall survival (OS) and time to progression (TTP) were evaluated with the C-index and the area under the curve for pathologic complete response.

Results: The best-performing baseline models for OS and TTP were based on the combination of SOURCE-cfDNA that reached a C-index of 0.55 and 0.59 compared with 0.44 to 0.45 with SOURCE alone. The addition of restaging positron emission tomography radiomics to SOURCE was the most promising addition for predicting OS (C-index: 0.65) and TTP (C-index: 0.60). Baseline risk stratification was achieved for OS and TTP by combining SOURCE with radiomics or cfDNA, log-rank $P <$ .01. The best-performing combination model for the prediction of pathologic complete response reached an area under the curve of 0.61 compared with 0.47 with SOURCE variables alone.

Conclusions: The addition of radiomics and cfDNA can improve the performance of an established survival model. External validity needs to be further assessed in future studies together with the optimization of radiomic pipelines.

Introduction

Currently, personalized outcome predictions to guide treatment for resectable esophageal adenocarcinoma (rEAC) are lacking.[1] One of the primary treatment modalities for rEAC involves neoadjuvant carboplatin and paclitaxel-based chemoradiation therapy (nCRT) according to CROSS and adjuvant nivolumab for incomplete responders.[2,3] This treatment regimen has shown improved survival compared with surgery alone, but locoregional and systematic relapses negatively impacts long-term outcome.[3,4] An established alternative for treating rEAC is perioperative chemotherapy according to the FLOT protocol.[5] The ESOPEC trial presented at ASCO 2024 compared FLOT with CROSS and found superior survival results for FLOT.[6] However, potentially the CROSS arm underperformed with a lower complete response rate and less patients able to finish the full protocol compared with historical data.[2] Moreover, perioperative chemotherapy is associated with more neutropenia and diarrhea based on data from the Neo-AEGIS trial.[7] Identifying patients who are likely to benefit from either CROSS or FLOT through prediction of survival or response could aid in selecting the most suitable candidates. Such an approach would not only benefit treated patients, but will also reduce health care costs and protect individuals from potential complications or side effects associated with ineffective treatments. To fulfill this purpose, models that integrate clinical characteristics, radiologic, and nuclear imaging as well as other biomarker data can be employed.

Routine medical imaging provides qualitative information, but it fails to capture the wealth of hidden information that is invisible to the human eye. Radiomics, involves extracting multiple additional features or combinations thereof, such as intensity, shape, and texture features, from the image voxels of both tumors and healthy tissue.[8-10] By leveraging radiomics alongside clinical data and other biomarkers, we can enhance our understanding of tumor biology, and develop prediction models to inform clinical decision making.[8] Several studies have found that handcrafted manual delineations and deep learning-derived radiomic feature extraction can be used to predict survival, therapy response, and adverse events, alone or in combination with biomarker and clinical data.[11-16] In head and neck squamous cell carcinoma and diffuse large B-cell lymphoma adding computed tomography (CT) or 2-deoxy-2-[^{18}F]fluoro-D-glucose ([^{18}F]FDG) positron emission tomography (PET) radiomic features to clinical or biological variables improved overall survival (OS) and 2-year time to progression (TTP) model estimates.[11,14] A recently conducted study in resectable esophageal cancer found an improvement in response prediction after adding data relating to the expression of the immunohistochemistry tumor markers Human Epidermal growth factor Receptor 2 and CD44 to clinico-radiomic models.[13] Other promising biomarkers such as tumor-derived cell-free DNA (cfDNA) from liquid biopsy can provide information on cancer detection, prognosis, treatment response, and targeted therapy.[17,18] In patients with rEAC, it has already been shown that cfDNA tumor fraction quantification and mutation detection is prognostic for survival but if it is a useful addition in clinico-radiomic models remains unknown.[19-22]

In our previous work, we developed the externally validated prediction model SOURCE for OS, using clinical variables from 13,080 patients obtained from the Netherlands Cancer Registry.[23,24] In this model, relevant baseline clinical parameters were identified from electronic health records specific for patients with esophageal cancer treated with curative intent. To further enhance personalized treatment predictions, we aim to explore the potential improvement in the SOURCE model's performance by integrating liquid biopsy and radiomics data. Therefore, in this exploratory retrospective study, we investigate whether the addition of radiomic and/or cfDNA features can enhance the predictive power of the SOURCE model for survival and response prediction.

Materials and Methods

In total, 111 patients with stage II-III (M0) resectable esophageal or gastroesophageal junction adenocarcinoma were included in this study treated consecutively between 2014 and 2019 in the Amsterdam UMC (n = 104) or UMC

Utrecht (n = 7). Neoadjuvant treatment consisted in 40 patients of neoadjuvant chemoradiation therapy according to CROSS (nCRT) combined with programmed death ligand 1 immune checkpoint inhibition and in 71 patients of nCRT only. The immune checkpoint inhibition-treated patients were part of a prospective phase 2 nonrandomized feasibility trial (PERFECT).[25] The patients who were enrolled in the PERFECT trial received neoadjuvant immunotherapy intravenous atezolizumab (1200 mg) concurrent with chemoradiation therapy in week 1 and week 4. Atezolizumab monotherapy was administered after neoadjuvant chemoradiation therapy in weeks 7, 10, and 13 before surgery. The nCRT only patients were included from the prospectively collected BIOES Amsterdam UMC biobank. All patients provided written, informed consent before study participation. This study was conducted in accordance with the Declaration of Helsinki and the international standards of good clinical practice.

SOURCE model clinical variables

For downstream analyses, the original linear predictor of the SOURCE survival prediction model for potentially curable esophageal cancer was used as reported earlier.[23] The linear predictor refers to the weighted sum of the covariates for each patient in the data, where the weights are the regression coefficients. The following baseline clinical variables on which the SOURCE model was based were extracted for the whole cohort: body mass index, albumin, hemoglobin, lactate dehydrogenase, age, clinical tumor stage, clinical nodal stage, tumor topography, and differentiation grade.[23]

Image acquisition and reconstruction from CT and [^{18}F]FDG-PET

From the complete cohort, baseline CT images used for diagnostic or radiation therapy treatment planning with comparable quality were available from 111 patients. Additionally, restaging CT scans after neoadjuvant treatment were available from 109 patients. Posttreatment imaging was performed with a median interval of 27 days (minimum 18 days to maximum 77 days) measured from the end of chemoradiation. The EANM Research limited-compliant [^{18}F]FDG-PET scans were available from 61 patients at baseline and from 105 at restaging.[26] The EANM Research limited guidelines help to ensure uniform imaging standards and enhance reproducibility. The scans were acquired and reconstructed according to standard operating procedures at the respective centers for diagnostic imaging.[26] The [^{18}F]FDG-PET instructions for patients included fasting for at least 6 hours before scanning. Serum glucose levels were measured and were in the range of 4 and 11 mmol/L. Acquisition of the PET scan was scheduled 60 ± 5 minutes after administration of an intravenous [^{18}F]FDG bolus of approximately 3 MBq/kg. Alongside the [^{18}F]FDG-PET, diagnostic CTs were made (5 mm slices, 3 mm reconstruction) with intravenous and oral contrast for the Amsterdam UMC patients and 5 mm reconstruction for patients treated in the UMC Utrecht. Manufacturers and respective convolution kernel reconstruction was from either Philips or Siemens for CT and PET. Except for the baseline CT scans of 10 patients that were acquired on a Toshiba (n = 5) or GE HealthCare scanner (n = 5). Additional information regarding patient and imaging characteristics according to the image biomarker standardization initiative reporting guidelines is given in Table E1.

Radiomic feature extraction and harmonization

For the CT images, manual delineation of the primary gross tumor volume (GTV) in MIM Maestro (MIM software) was performed by T.v.d.E. and peer-reviewed by Y.W. The GTV delineation was adjusted according to the radiology or endoscopic ultrasound report. In cases with available [^{18}F]FDG-PET scans, they were used in conjunction to guide the delineation. In total 105 radiomic features were extracted from the GTV using the PyRadiomics Python package version 3.01.[27] The extracted quantitative metrics were 14 shape features from the region of interest, 18 intensity features, and 73 texture features (22 derived from the gray level co-occurrence matrix [glcm], 16 from the gray level run length matrix [glrlm], 16 from the gray level size zone matrix [glszm], 14 from the gray level dependence matrix [gldm], and 5 from the neighboring gray tone difference matrix [ngtdm]). The radiomic feature "original_shape_VoxelVolume" was regarded as a proxy marker for tumor volume. Additionally, the [^{18}F]FDG-PET images were used for the same radiomic feature extraction based on the primary esophageal tumor volume of interest. The volume of interest delineation was performed in 3DSlicer version 4.11 (www.slicer.org) and in-house built software implemented in Python 3.7.2 (Python Software Foundation).[28] Boxing was applied to exclude surrounding [^{18}F]FDG-avid tissues. Esophageal primary tumor location was delineated using an isocontour that applies an adaptive threshold of 50% of the SUVpeak, obtained using a sphere of 12 mm diameter, corrected for local background.[29,30] At baseline there were less than 100 PET scans available (n = 61) and were therefore not used for radiomic analysis.[31] Only the restaging, PET scans made after neoadjuvant therapy were used (n = 105). For the radiomic feature extraction in PyRadiomics, a fixed bin size of 0.5 g/mL was used for PET and 25 HU for CT. The interpolator used for resampling was sitkBSpline. The pixel spacing was set to ($4 \times 4 \times 4$ mm^3) for PET and ($1 \times 1 \times 1$ mm^3) for CT in PyRadiomics. The surrogate variable analysis R package (version 3.38.0) was used for ComBat post-processing harmonization to correct for the 2 main sources of data variability namely: convolution kernel reflected by manufacturer (Philips, Siemens, Toshiba, GE Healthcare) and slice thickness (3 mm or less vs 4-5 mm).[32-34] This post-processing using ComBat ensured that the variability of the convolution kernel and slice thickness due to

different manufacturers was accounted for and removed any unwanted variability that was not due to tumor-related differences. This was done for CT baseline, CT posttreatment, and PET posttreatment.

Liquid biopsy cfDNA metrics

Details on blood plasma collection, DNA isolation, library preparation, and sequencing have previously been published.[35,36] For this study we only used baseline cfDNA features and tumor agnostic mutation data. In short, blood samples were collected into EDTA tubes and processed with double-centrifugation (1600 g for 10 minutes and 16,000 g for 10 minutes) before storage at −80°C. Plasma cfDNA was extracted using QIAGEN kits. Baseline liquid biopsy data were derived from shallow whole-genome sequencing <1 × depth of coverage on a NovaSeq 6000 and an esophageal adenocarcinoma ion-torrent amplicon targeted gene panel (23 genes).[18,21,37] Library preparation of the amplicon panel was performed according to the standard operating procedure of the Ion AmpliSeq HD Library Kit and the Ion AmpliSeq HD Dual Barcode kit with 5 ng of input per pool. Sequencing of libraries was done on the Ion S5 NGS system. The mean base coverage depth for cfDNA samples was 10,524 × and for white blood cell samples 9647 × . The following cfDNA metrics were used to estimate tumor fraction from shallow whole-genome sequencing: short fragments (P20-150), somatic copy number aberrations (IchorCNA), and fragment end sequence score as previously described.[35,36] The amplicon sequencing results corrected for white blood cell variants were used for the detection of mutations.

Clinical outcomes

The following outcome measures were used: OS, TTP, and pathological complete response (pCR; ypT0N0). OS was defined as the days elapsed from start of treatment until death or censored at the end of follow-up, and for TTP until disease progression, recurrence, or censored at the end of follow-up. Data cutoff for OS and TTP was January 14, 2022. pCR was a binary outcome comparing complete responders with patients with residual disease or pre-surgery progression. The SOURCE model, radiomic features, and cfDNA metrics served as input for the different prediction models constructed for these 3 outcomes (OS, TTP, and pCR) (Fig. 1A). Models were first constructed to predict each outcome based on the single input of SOURCE, baseline or restaging radiomics or cfDNA. Thereafter, double parameter models were constructed by combining SOURCE with radiomics or cfDNA. Finally, all 3 parameters were combined and compared with the different radiomic combinations (baseline CT, restaging CT, and restaging PET).

Statistical analysis

Before predictive modeling, for each timepoint (baseline and follow-up) and scan-type (CT and PET) an initial feature selection of the 105 radiomic features was performed to remove highly correlating features (≥0.75) using the redundancy filter algorithm based on a Spearman correlation matrix within the FMradio (Factor Modelling for Radiomics Data) R package (version 1.1.1).[38] After removing the highly correlated features, between 28 and 34 were left depending on timepoint and scan-type. Next, elastic net regularization from the glmnet R package (version 4.1-7) was used to develop the prediction models for OS, TTP, and pCR using clinical, cDNA, and radiomic features as predictors.[39] Elastic net is a linear regression regularization technique that combines Lasso (L1) and Ridge (L2) penalties. It balances sparsity (zero coefficients) and shrinkage (small coefficients) using 2 parameters, lambda and alpha, offering a flexible approach to improve model performance and handle correlated features. Consequently, elastic net also performs feature selection. OS and TTP were modeled using an elastic net Cox regression and pCR was modeled using a logistic elastic net regression. The lambda parameter and alpha penalty mixing parameter were optimized using a 10-fold cross-validation scheme (Fig. 1B). Across all models, feature selection was handled via elastic net modeling.

Predictors in each model included the redundancy filtered radiomic features, a predefined set of 4 cfDNA metrics reflective of tumor fraction: short fragments P20-150 (dichotomous; threshold 0.2), ichorCNA (dichotomous; threshold 0.3), fragment end sequence score (continuous parameter), and mutation (dichotomous; threshold VAF 1%), the linear predictor or clinical variables from the SOURCE prediction model, and all respective combinations. Missing data on clinical variables were handled and imputed with a random forest imputation using the missRanger package in R (version 2.2.1).[40] For the time-to-event models (OS and TTP), the linear predictor of the SOURCE prediction model was used as a single predictor to reflect the clinical variables. Using the linear predictor, the original covariances of the original SOURCE model remained intact. For logistic models (pCR), all clinical variables from the SOURCE prediction model were used in the modeling procedure as the linear prediction was developed in the context of a Cox regression model as opposed to a logistic regression model. Additionally, an exploratory analysis was performed for pCR by using the delta radiomic values from matched baseline and restaging CT scans (restaging value−baseline value).

For time-to-event models, the concordance (C-index) was used to assess predictive performance and the area under the curve (AUC)-Receiver Operator Curve (ROC) to evaluate performance of the logistic models. In the context for survival models, the C-index expresses whether the models can distinguish between patients with low-risk and high-risk of an event.[41] A C-index of 0.5 indicates poor

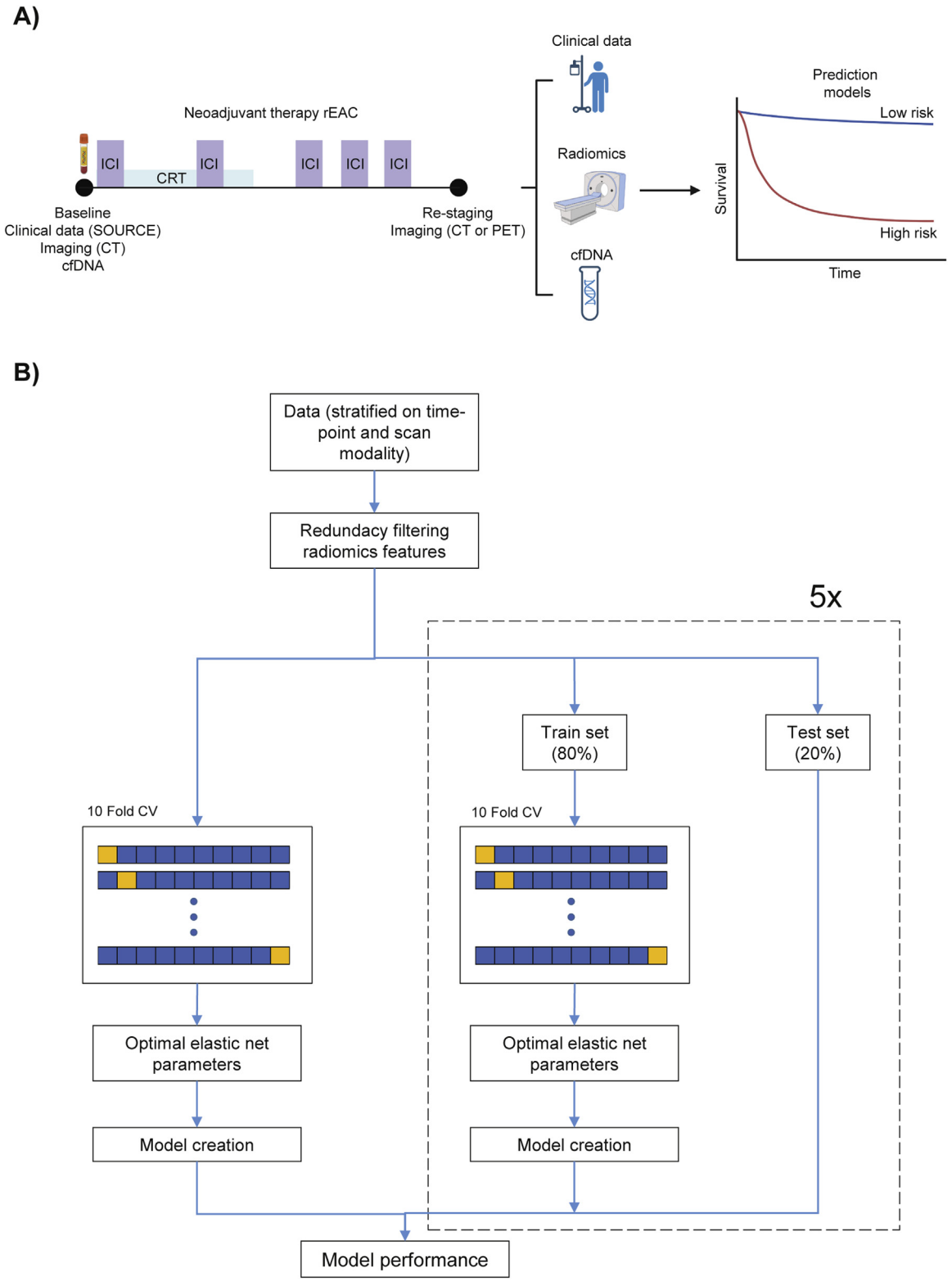

Fig. 1. Study method for developing predictions for survival and pathologic response. (A) Treatment schedule of patients included in this study. Patients were treated with neoadjuvant chemoradiation therapy (nCRT) and a subset of patients also received neoadjuvant immune checkpoint inhibition (ICI). The predictions for survival and response are based on radiomics, SOURCE, and cfDNA. (B) Elastic net regression analysis with cross-validation method. *Abbreviation:* cfDNA = cell-free DNA; CT = computed tomography; PET = positron emission tomography; CV = Cross-Validation.

discrimination and 1.0 indicates perfect discrimination. For logistic models, the AUC expresses whether models can discriminate between patients with and without a pathologically complete response.[42] An AUC of 0.5 indicates poor discrimination and 1.0 indicates perfect discrimination. Both the C-index and AUC provide an indication of the model' ability to discriminate between patients with short and long survival or detect a higher likelihood of pCR. Given the explorative nature of this study, these metrics were chosen as the primary metric to evaluate all models on.

Bootstrapping (500 iterations) was used to empirically estimate 95% confidence intervals for the performance metrics. Furthermore, for every fitted prediction model, we performed an internal-external 5-fold cross-validation to assess performance of the model on data on which the model was not trained (80% training and 20% validation). In each fold, the entire modeling pipeline was repeated. Finally, a random permutation test of the outcomes was performed to investigate overfitting (Table E1).[43] The values obtained by cross-validation were the primary outcome of this study, as these would better reflect the external reproducibility.

On the basis of the fitted models, we constructed Kaplan-Meier curves of the time-to-event models and ROC curves of the logistic models. For the Kaplan-Meier curves, patients were classified into low-risk and high-risk groups based on the linear predictor values of each patient from the fitted model. The optimal cut point for the determination of high-risk and low-risk was optimized by finding the maximum rank statistic (prognostic index).[44] A log-rank test was used to statistically test the 2 arms of the curve. For this study the TRIPOD statement (transparent reporting of multivariable prediction model for individual prognosis or diagnosis, version October 1, 2020) can be found in Table E2.[45]

Results

Prediction models for survival and disease progression

Table 1 displays all clinical characteristics of patients included in this study. Survival models were constructed based on 3 different types of data: the linear predictor of SOURCE, radiomics (CT or PET), and cfDNA data. The apparent C-indices derived from Cox regression analysis on the full dataset (apparent) and 5-fold cross-validated estimates are given in Figure 2. Below we report the cross-validated results as these are most representative for external performance. The C-index of the clinical model (SOURCE) for OS was 0.45 (Fig. 2A). The addition of baseline CT radiomics or cfDNA to the clinical model improved the C-indices to 0.54 and 0.55, respectively. Combining all 3 baseline metrics did not lead to any additional improvement, as SOURCE, CT radiomics, and cfDNA reached a C-index of 0.54. Baseline features selected in the CT radiomic models were 2 features namely: gldm_SmallDependenceEmphasis and ngtdm_Strength. Additionally, we assessed if the

Table 1 Baseline characteristics and clinical response from the 111 included patients

Variable	Absolute number, n	%
Age (y)		
Median (range)	64 (35-75)	-
Sex		
Male	98	88.3
Female	13	11.7
Body mass index*		
Median (range)	26.2 (17-40.3)	-
Clinical tumor stage		
cT1	1	0.9
cT2	24	21.6
cT3	83	74.8
cT4a	2	1.8
cTx	1	0.9
Clinical nodal stage		
cN0	33	29.7
cN1	50	45
cN2	26	23.4
cN3	2	1.8
Tumor topography		
Proximal	1	0.9
Mid	3	2.7
Distal	85	76.6
GEJ	22	19.8
Differentiation		
Well	4	3.6
Moderate	46	41.4
Poor	38	34.2
Not recorded	23	20.7
Laboratory values†		
Albumin (n = 75)	43 (29-49)	-
Hemoglobin (n = 110)	8.8 (5.7-10.7)	-
LDH (n = 107)	180 (110-266)	-
Neoadjuvant therapy		
nCRT	71	64
nCRT+anti-PD-L1	40	36
Pathological response		
pCR	25	22.5
Non-pCR (ypT+ or ypN+)	78	70.3
Preoperative progression	5	4.5
No surgery (reason other)	3	2.7

Abbreviations: cN = clinical nodal stage; cT = clinical tumor stage; GEJ = gastroesophageal junction; LDH = lactate dehydrogenase; nCRT = neoadjuvant chemoradiation therapy; PD-L1 = programmed death ligand 1; TRG = tumor regression grade.

* For 1 patient, there were no data available to calculate body mass index.

† In brackets the number of patients is given from whom the baseline value was available. Median and range are given for laboratory values.

restaging CT- or PET-derived radiomic features could be used for OS prediction together with the clinical model and/or cfDNA. The addition of restaging PET radiomics to the clinical model improved the C-index for OS to 0.65 that was better than the addition of restaging CT radiomics (C-index: 0.48). The addition of cfDNA to the clinico-radiomic restaging PET model did not improve the C-index (0.62) (Fig. 2A). The features selected in the PET models were 3 features namely: firstorder_Skewness, gldm_DependenceNonUniformity, and ngtdm_Contrast. The complete overview of selected features for each model and coefficients are given in Table E3. These findings suggest that the addition of radiomic features or cfDNA can improve the performance of an established OS model such as SOURCE.

Next, we investigated the performance of different models for the prediction of TTP (Fig. 2B). Below we report the 5-fold cross-validated estimates. The C-index for the clinical model (SOURCE) was 0.44 (Fig. 2B). The addition of baseline CT radiomics or cfDNA to the clinical model improved the C-indices to 0.55 and 0.59, respectively. Combining all 3 baseline metrics SOURCE, CT radiomics, and cfDNA reached a C-index of 0.56 that was not better than the SOURCE-cfDNA model (Fig. 2B). Baseline CT features selected were glrlm_RunEntropy, gldm_SmallDependenceEmphasis, ngtdm_Coarseness, and ngtdm_Strength. Additionally, we assessed if the restaging CT- or PET-derived radiomic features could be used for TTP prediction together with the clinical model and/or cfDNA. The addition of restaging PET radiomics to the clinical model improved the C-index for TTP to 0.60 that was better than the addition of restaging CT radiomics (C-index: 0.45). The addition of cfDNA to the clinico-radiomic restaging PET model did not improve the C-index (0.59) (Fig. 2B). The features selected in the PET models were firstorder_Skewness, glcm_Idmn, gldm_DependenceNonUniformity, and ngtdm_Contrast. The complete overview of selected features for each model and coefficients are given in Table E3. The prediction of TTP could thus be enhanced by adding radiomics or cfDNA to the clinical SOURCE model.

To investigate if these models could be used for baseline risk stratification we performed an exploratory analysis by Kaplan-Meier analysis of the prognostic index by only using baseline metrics (SOURCE, baseline CT radiomics, and cfDNA). For both OS and TTP, it was possible to identify a high- and low-risk group after determining the optimal cut-off point of the prognostic index for each model (Fig. 3). Similar stratification for OS was achieved by the SOURCE-radiomics (Fig. 3B) and SOURCE-radiomics-cfDNA model, log-rank $P = .0017$ (Fig. 3D). For TTP, the SOURCE-radiomics-cfDNA model was able to provide the best separation of the Kaplan-Meier curve, log-rank $P = .0001$ (Fig. 3H). Risk stratification could thus be achieved by combining SOURCE with radiomics or cfDNA metrics.

Prediction models for treatment response

To predict pCR after neoadjuvant therapy, we compared the performance of AUC classification based on SOURCE, cfDNA, and radiomics from baseline or restaging imaging (Fig. 4). Below we report the 5-fold cross-validated estimates. First, we investigated if baseline CT-derived radiomics can be used in combination with other metrics to predict pCR. The classification of response with only the SOURCE variables reached an AUC of 0.47 (Fig. 4). The combination model of SOURCE with baseline CT radiomics improved the AUC to 0.61, whereas this was not seen with the addition of cfDNA to SOURCE, AUC: 0.48. Combining all 3 baseline metrics SOURCE, CT radiomics, and cfDNA reached an AUC of 0.61. Baseline features in the CT radiomic models were among others: glrlm_RunEntropy, glszm_SizeZoneNonUniformity, gldm_DependenceEntropy, gldm_SmallDependenceEmphasis, and ngtdm_Busyness. Next, we assessed if the restaging CT- or PET-derived radiomic features could be used for pCR prediction together with the clinical variables and/or cfDNA. The addition of restaging CT or PET radiomics to the SOURCE variables did not lead to any meaningful improvement with AUCs of

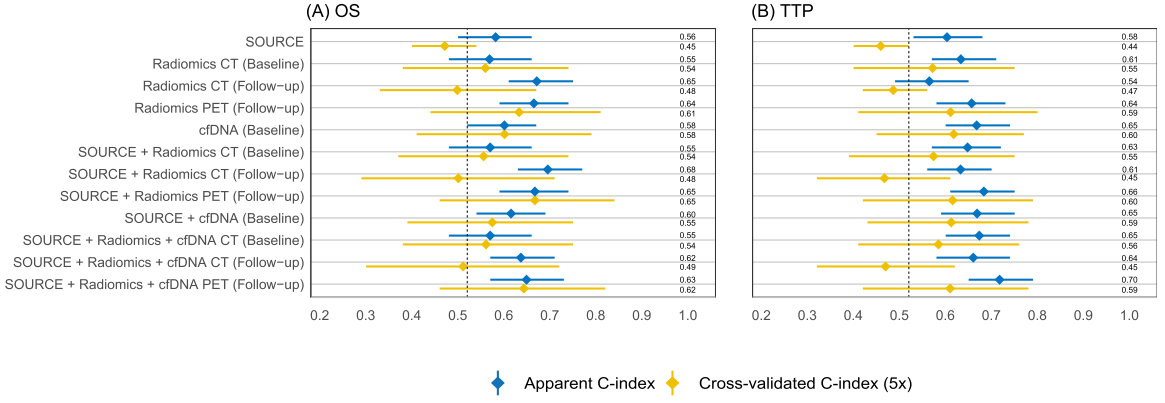

Fig. 2. Prediction models for (A) OS and (B) TTP with in blue the apparent C-indices and in yellow the cross-validated estimates. *Abbreviations:* cfDNA = cell-free DNA; CT = computed tomography; OS = overall survival; PET = positron emission tomography; TTP = time to progression.

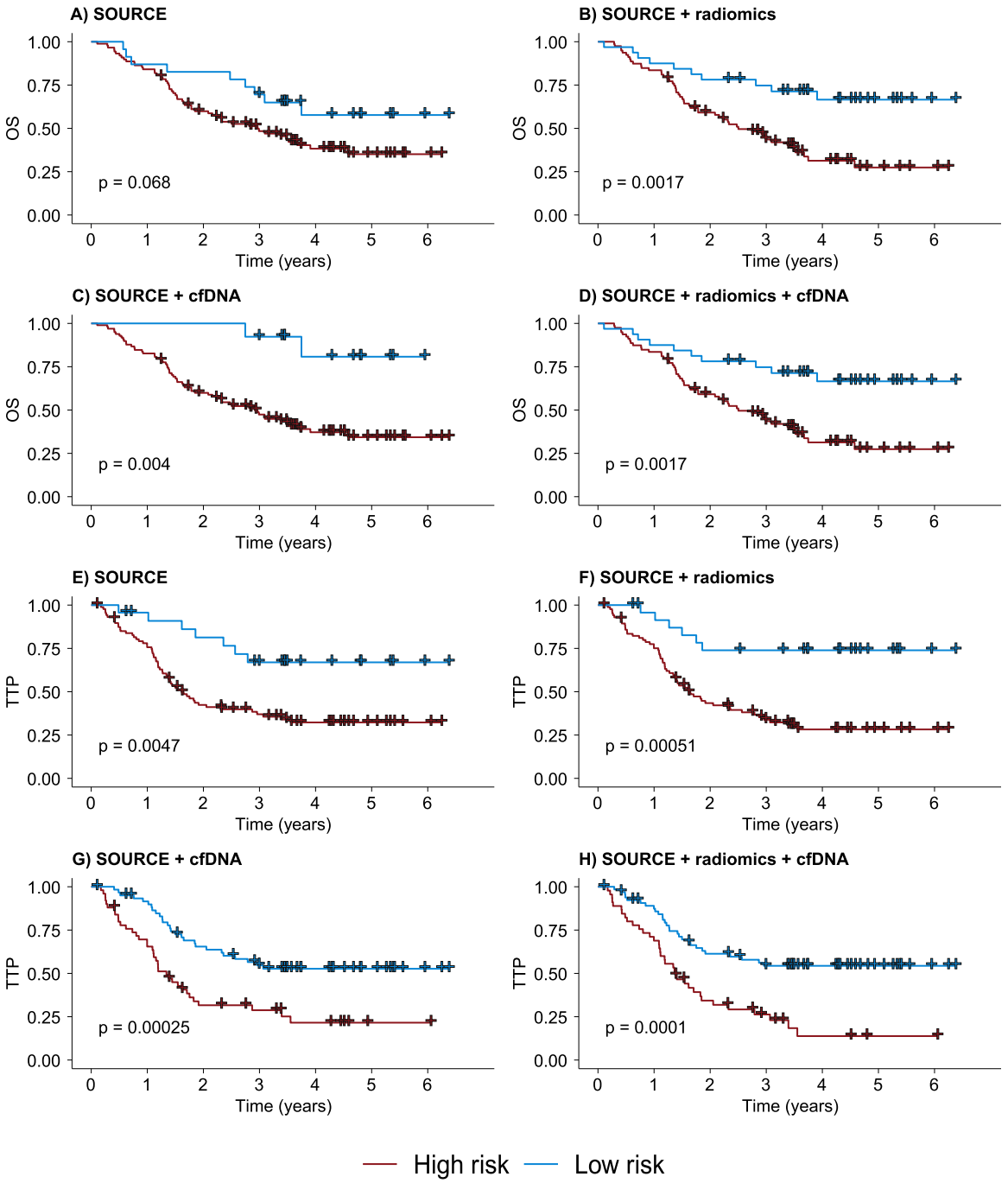

Fig. 3. Baseline risk stratification by Kaplan-Meier for OS (A-D) and TTP (E-H). *Abbreviations:* cfDNA = cell-free DNA; OS = overall survival; TTP = time to progression.

0.49 and 0.42, respectively (Fig. 4). The combination of all 3, SOURCE, restaging CT or PET, and cfDNA, was also of no additional value with AUCs of 0.50 and 0.42. An exploratory analysis of delta CT radiomics alone or together with the SOURCE variables and/or cfDNA reached AUCs after cross-validation between 0.37 and 0.44 (Fig. 4). The only features selected in the delta radiomic models was glszm_ZoneEntropy. The complete overview of selected features for each model and coefficients are given in Table E3. In conclusion, the prediction of pCR improves after combining the SOURCE variables, baseline CT radiomics, and baseline cfDNA data compared with clinical variables alone.

Discussion

This study evaluated whether integrating clinical variables, radiomics, and tumor-derived cfDNA data can improve survival and response prediction for patients with rEAC treated

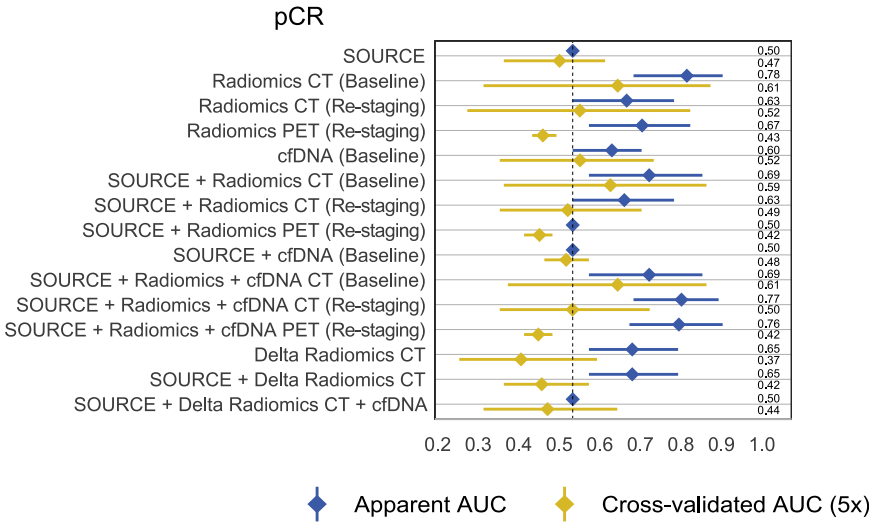

Fig. 4. Classification of pCR with in blue the apparent AUCs and in yellow the cross-validated estimates. *Abbreviations:* AUC = area under the curve; CT = computed tomography; pCR = pathologic complete response; PET = positron emission tomography.

in the neoadjuvant setting compared with the clinical SOURCE model alone. The addition of cfDNA or CT radiomics to the clinical SOURCE model was able to improve baseline prediction models for OS and TTP. However, the cross-validated estimates were relatively low. Baseline risk stratification for survival was possible based on the prognostic index of the regression models. Restaging PET radiomics was the most promising addition to the clinical SOURCE model. The addition of baseline CT radiomics and cfDNA to clinical variables was able to marginally improve the prediction of pCR compared with clinical variables alone.

Several studies in different cancer types have found that radiomics can improve upon conventional staging or clinical variables.[10,14,46,47] Most studies on radiomics use a select number of clinical variables including among others the American Joint Committee on Cancer staging system. In our proof-of-concept study, we were able to improve the performance of the clinical SOURCE model by adding cfDNA or handcrafted radiomic features. Moreover, baseline regression models were able to classify patients into a high and low survival group. It must however be noted that despite the observed improvement, the cross-validated C-indices were relatively low ≤0.65 and are thus not yet ready for clinical implementation. As a next step, external validation and optimization in larger cohorts will be necessary. Unfortunately, analyzing large datasets in radiomics is a time-consuming process partly due to the manual delineation step. A potential solution to this problem is automatic segmentation that can help speed up delineation, improve accuracy, and provide better risk stratification. A recently conducted study in lung cancer showed faster and better reproducible delineations by an automated pipeline.[48] Moreover, in the majority of cases, the radiologist or radiation oncologist preferred the automated segmentation compared with the manually delineated volume.[48] Other techniques that can improve radiomics performance are combining handcrafted radiomics and deep learning algorithms with ensemble learning or consensus algorithms.[49] This has already led to improvements in the classification of idiopathic pulmonary fibrosis and prediction of adverse radiation effects in patients with brain metastases.[16,50] Our study provides support for the continued investigation of these techniques for radiomic feature extraction, and data analysis alongside integration into gastroesophageal prognostic models such as SOURCE.[23] Future studies should consider addressing certain aspects, such as enhancing preprocessing techniques and incorporating additional harmonization methods like ComBat, as utilized in our study.[51]

This study observed that baseline cfDNA biomarker data were of additive value for the prediction of OS or TTP together with SOURCE and/or radiomics. Previous studies were also able to establish the additional value of combining genomic or pathology biomarkers with clinical data and radiomics.[13,52-54] In a non-small cell lung cancer study, the addition of cfDNA data to a clinico-radiomic model improved the prediction of survival models in patients with metastatic treated with epidermal growth factor receptor targeted therapy.[53] The combination of baseline cfDNA metrics and SOURCE showed better capacity to inform on TTP (C-index: 0.59) than OS (C-index: 0.55). Other studies also found that cfDNA was a marker for progression at baseline or at later timepoints in rEAC.[19,20,55,56] Current results do not support the integration of cfDNA into rEAC-specific survival models as it is not yet sufficiently informative regarding OS prediction and TTP. Also, cfDNA analysis is relatively expensive, whereas radiomics uses readily available diagnostic imaging. In our models we only used baseline cfDNA data and used a tumor agnostic approach. To

further improve the utility of cfDNA profiling, repeated sampling or sequencing for methylation changes may improve prognostication.[20,57] Several other biomarkers in esophageal cancer detected in blood or tissue could be included in predictive models.[58,59] For example, the presence of tumor-associated immune cells in the tumor microenvironment was predictive of nCRT response.[60] Molecular characterization by subtyping esophageal cancer could help stratify patients for certain treatments such as immunotherapy for the microsatellite instable tumors.[61,62] Moving forward, these biomarkers that can technically be implemented in patient care need to be further evaluated if they can improve clinical prediction models such as SOURCE.

In our study the restaging PET radiomics were the most promising addition to the clinical SOURCE model. From a clinical perspective, baseline models would be preferred to select patients upfront for certain treatments and this can be combined with for example baseline immune profiling of the TME to predict response to chemoradiation.[63] Incorporating non-baseline measurements into these decision systems may nevertheless be of value to select patients for surgery after restaging imaging in patients with rEAC. Putting our results into context of current literature, longitudinal radiomic features were able to predict patient outcome in several tumor types.[64-67] A recently conducted systematic review highlights its advantages but also its limitations, especially regarding the heterogeneous methods used within each paper.[65] On the basis of our study, further exploration of adding longitudinal imaging radiomics for personalized outcome prediction seems more promising than only baseline measurements, although the difference was small between baseline and restaging models. Features from the best-performing restaging PET model for OS were related to voxel skewness, local intensity variation between neighboring voxels, and gray level homogeneity. Interestingly, a previous study in non-small cell lung cancer also found skewness, as a PET radiomic feature, to be associated with a higher chance of progression after immunotherapy.[68] These features could be related to the degree of tissue heterogeneity and need further biological validation.[69] In conclusion, our results support the further development of longitudinal radiomic models in decision support systems.[70,71]

In this study, there were several methodological limitations worth considering. Because of the relatively small sample size of the cohort, the risk of overfitting was present. Cross-validation was used to investigate this and revealed that the cross-validated point estimates were generally significantly lower than the apparent estimates. This suggests that further external validation will be necessary. Another limitation is the use of the linear predictor from SOURCE for TTP, whereas it was originally developed for OS. This was based on the assumption that the covariance structure of the SOURCE model would also be valid for modeling TTP. However, as SOURCE was never validated for TTP, we could not test this assumption. In this study we were also not able to look separately at patients treated with or without immunotherapy as the numbers were too small for separate analyses.

Conclusions

Clinical survival prediction models such as SOURCE could be improved by integrating radiomics or cfDNA measurements. Moreover, the addition of restaging radiomic PET features to a clinical model was promising to predict OS and TTP. The prediction of pCR improved after adding baseline CT radiomic features and cfDNA to the SOURCE variables. However, currently developed models are not yet sufficient for clinical implementation due to possibly poor external validity. Future studies should explore the optimization of radiomic pipelines, eg, integrating handcrafted and deep radiomics, in personalized prognostic predictions or treatment stratification for rEAC.

References

1. Obermannová R, Alsina M, Cervantes A, et al. Oesophageal cancer: ESMO clinical practice guideline for diagnosis, treatment and follow-up. *Ann Oncol* 2022;33:992-1004.
2. van Hagen P, Hulshof MC, van Lanschot JJ, et al. Preoperative chemoradiotherapy for esophageal or junctional cancer. *N Engl J Med* 2012;366:2074-2084.
3. Kelly RJ, Ajani JA, Kuzdzal J, et al. Adjuvant nivolumab in resected esophageal or gastroesophageal junction cancer. *N Engl J Med* 2021;384:1191-1203.
4. Shapiro J, van Lanschot JJB, Hulshof M, et al. Neoadjuvant chemoradiotherapy plus surgery versus surgery alone for oesophageal or junctional cancer (CROSS): Long-term results of a randomised controlled trial. *Lancet Oncol* 2015;16:1090-1098.
5. Al-Batran SE, Homann N, Pauligk C, et al. Perioperative chemotherapy with fluorouracil plus leucovorin, oxaliplatin, and docetaxel versus fluorouracil or capecitabine plus cisplatin and epirubicin for locally advanced, resectable gastric or gastro-oesophageal junction adenocarcinoma (FLOT4): A randomised, phase 2/3 trial. *Lancet* 2019;393:1948-1957.
6. Hoeppner J, Brunner T, Lordick F, et al. Prospective randomized multicenter phase III trial comparing perioperative chemotherapy (FLOT protocol) to neoadjuvant chemoradiation (CROSS protocol) in patients with adenocarcinoma of the esophagus (ESOPEC trial). *J Clin Oncol* 2024;42 LBA1-LBA.
7. Reynolds JV, Preston SR, O'Neill B, et al. Trimodality therapy versus perioperative chemotherapy in the management of locally advanced adenocarcinoma of the oesophagus and oesophagogastric junction (Neo-AEGIS): An open-label, randomised, phase 3 trial. *Lancet Gastroenterol Hepatol* 2023;8:1015-1027.
8. Lambin P, Leijenaar RTH, Deist TM, et al. Radiomics: The bridge between medical imaging and personalized medicine. *Nat Rev Clin Oncol* 2017;14:749-762.
9. Lambin P, Rios-Velazquez E, Leijenaar R, et al. Radiomics: Extracting more information from medical images using advanced feature analysis. *Eur J Cancer* 2012;48:441-446.
10. Aerts HJ, Velazquez ER, Leijenaar RT, et al. Decoding tumour phenotype by noninvasive imaging using a quantitative radiomics approach. *Nat Commun* 2014;5:4006.
11. Eertink JJ, van de Brug T, Wiegers SE, et al. ^{18}F-FDG PET baseline radiomics features improve the prediction of treatment outcome in

diffuse large B-cell lymphoma. *Eur J Nucl Med Mol Imaging* 2022;49:932-942.
12. Beukinga RJ, Poelmann FB, Kats-Ugurlu G, et al. Prediction of non-response to neoadjuvant chemoradiotherapy in esophageal cancer patients with ^{18}F-FDG PET radiomics based machine learning classification. *Diagnostics (Basel)* 2022;12:1070.
13. Beukinga RJ, Wang D, Karrenbeld A, et al. Addition of HER2 and CD44 to ^{18}F-FDG PET-based clinico-radiomic models enhances prediction of neoadjuvant chemoradiotherapy response in esophageal cancer. *Eur Radiol* 2021;31:3306-3314.
14. Keek SA, Wesseling FWR, Woodruff HC, et al. A prospectively validated prognostic model for patients with locally advanced squamous cell carcinoma of the head and neck based on radiomics of computed tomography images. *Cancers (Basel)* 2021;13:3271.
15. Salahuddin Z, Chen Y, Zhong X, Rad NM, Woodruff HC, Lambin P. *HNT-AI: An Automatic Segmentation Framework for Head and Neck Primary Tumors and Lymph Nodes in FDG-PET/CT Images*. Springer Nature Switzerland; 2023:212-220.
16. Keek SA, Beuque M, Primakov S, et al. Predicting adverse radiation effects in brain tumors after stereotactic radiotherapy with deep learning and handcrafted radiomics. *Front Oncol* 2022;12 920393.
17. Dang DK, Park BH. Circulating tumor DNA: Current challenges for clinical utility. *J Clin Invest* 2022;132 e154941.
18. Mouliere F, Chandrananda D, Piskorz AM, et al. Enhanced detection of circulating tumor DNA by fragment size analysis. *Sci Transl Med* 2018;10:eaat4921.
19. Ococks E, Frankell AM, Masque Soler N, et al. Longitudinal tracking of 97 esophageal adenocarcinomas using liquid biopsy sampling. *Ann Oncol* 2021;32:522-532.
20. Ococks E, Sharma S, Ng AWT, Aleshin A, Fitzgerald RC, Smyth E. Serial circulating tumor DNA detection using a personalized, tumor-informed assay in esophageal adenocarcinoma patients following resection. *Gastroenterology* 2021;161:1705-1708 e2.
21. Moldovan N, van der Pol Y, van den Ende T, et al. Multi-modal cell-free DNA genomic and fragmentomic patterns enhance cancer survival and recurrence analysis. *Cell Rep Med* 2024;5:101349.
22. Wallander K, Eisfeldt J, Lindblad M, et al. Cell-free tumour DNA analysis detects copy number alterations in gastro-oesophageal cancer patients. *PLoS One* 2021;16 e0245488.
23. van den Boorn HG, Abu-Hanna A, Haj Mohammad N, et al. SOURCE: Prediction models for overall survival in patients with metastatic and potentially curable esophageal and gastric cancer. *J Natl Compr Canc Netw* 2021;19:403-410.
24. van Kleef JJ, van den Boorn HG, Verhoeven RHA, et al. External validation of the Dutch SOURCE survival prediction model in Belgian metastatic oesophageal and gastric cancer patients. *Cancers (Basel)* 2020;12:834.
25. van den Ende T, de Clercq NC, van Berge Henegouwen MI, et al. Neoadjuvant chemoradiotherapy combined with atezolizumab for resectable esophageal adenocarcinoma: A single-arm Phase II feasibility trial (PERFECT). *Clin Cancer Res* 2021;27:3351-3359.
26. Boellaard R, Delgado-Bolton R, Oyen WJ, et al. FDG PET/CT: EANM procedure guidelines for tumour imaging: Version 2.0. *Eur J Nucl Med Mol Imaging* 2015;42:328-354.
27. van Griethuysen JJM, Fedorov A, Parmar C, et al. Computational radiomics system to decode the radiographic phenotype. *Cancer Res* 2017;77:e104-e107.
28. Fedorov A, Beichel R, Kalpathy-Cramer J, et al. 3D slicer as an image computing platform for the quantitative imaging network. *Magn Reson Imaging* 2012;30:1323-1341.
29. Wahl RL, Jacene H, Kasamon Y, Lodge MA. From RECIST to PERCIST: Evolving considerations for PET response criteria in solid tumors. *J Nucl Med* 2009;50:122S-150S.
30. Frings V, van Velden FH, Velasquez LM, et al. Repeatability of metabolically active tumor volume measurements with FDG PET/CT in advanced gastrointestinal malignancies: A multicenter study. *Radiology* 2014;273:539-548.
31. Orlhac F, Nioche C, Klyuzhin I, Rahmim A, Buvat I. Radiomics in PET imaging: A practical guide for newcomers. *PET Clin* 2021;16:597-612.
32. Leek JT, Johnson WE, Parker HS, Jaffe AE, Storey JD. The sva package for removing batch effects and other unwanted variation in high-throughput experiments. *Bioinformatics* 2012;28:882-883.
33. Johnson WE, Li C, Rabinovic A. Adjusting batch effects in microarray expression data using empirical Bayes methods. *Biostatistics* 2007;8:118-127.
34. Ligero M, Jordi-Ollero O, Bernatowicz K, et al. Minimizing acquisition-related radiomics variability by image resampling and batch effect correction to allow for large-scale data analysis. *Eur Radiol* 2021;31:1460-1470.
35. Moldovan N, van der Pol Y, van den Ende T, et al. Multi-modal cell-free DNA genomic and fragmentomic patterns enhance cancer survival and recurrence analysis. *Cell Rep Med* 2024;5 101349.
36. van den Ende T, van der Pol Y, Creemers A, et al. Genome-wide and panel-based cell-free DNA characterization of patients with resectable esophageal adenocarcinoma. *J Pathol* 2023;261:286-297.
37. van der Pol Y, Moldovan N, Verkuijlen S, et al. The effect of preanalytical and physiological variables on cell-free DNA fragmentation. *Clin Chem* 2022;68:803-813.
38. Peeters CFW ÜC, Mes SW. Stable prediction with radiomics data. *ArXiv*. 2019:2019;abs/1903.11696.
39. Friedman JH, Hastie T, Tibshirani R. Regularization paths for generalized linear models via coordinate descent. *J Stat Softw* 2010;33:1-22.
40. Stekhoven DJ, Bühlmann P. MissForest—non-parametric missing value imputation for mixed-type data. *Bioinformatics* 2012;28:112-118.
41. Longato E, Vettoretti M, Di Camillo B. A practical perspective on the concordance index for the evaluation and selection of prognostic time-to-event models. *J Biomed Inform* 2020;108 103496.
42. de Hond AAH, Steyerberg EW, van Calster B. Interpreting area under the receiver operating characteristic curve. *Lancet Digit Health* 2022;4:e853-e855.
43. Buvat I, Orlhac F. The dark side of radiomics: On the paramount importance of publishing negative results. *J Nucl Med* 2019;60:1543-1544.
44. Royston P, Altman DG. External validation of a Cox prognostic model: Principles and methods. *BMC Med Res Methodol* 2013;13:33.
45. Collins GS, Reitsma JB, Altman DG, Moons KG. Transparent reporting of a multivariable prediction model for individual prognosis or diagnosis (TRIPOD): The TRIPOD statement. *BMJ* 2015;350:g7594.
46. Mossinelli C, Tagliabue M, Ruju F, et al. The role of radiomics in tongue cancer: A new tool for prognosis prediction. *Head Neck* 2023;45:849-861.
47. Li W, Zhang L, Tian C, et al. Prognostic value of computed tomography radiomics features in patients with gastric cancer following curative resection. *Eur Radiol* 2019;29:3079-3089.
48. Primakov SP, Ibrahim A, van Timmeren JE, et al. Automated detection and segmentation of non-small cell lung cancer computed tomography images. *Nat Commun* 2022;13:3423.
49. Rogers W, Thulasi Seetha S, Refaee TAG, et al. Radiomics: From qualitative to quantitative imaging. *Br J Radiol* 2020;93 20190948.
50. Refaee T, Salahuddin Z, Frix AN, et al. Diagnosis of idiopathic pulmonary fibrosis in high-resolution computed tomography scans using a combination of handcrafted radiomics and deep learning. *Front Med (Lausanne)* 2022;9 915243.
51. Mali SA, Ibrahim A, Woodruff HC, et al. Making radiomics more reproducible across scanner and imaging protocol variations: A review of harmonization methods. *J Pers Med* 2021;11:842.
52. Fathi Kazerooni A, Saxena S, Toorens E, et al. Clinical measures, radiomics, and genomics offer synergistic value in AI-based prediction of overall survival in patients with glioblastoma. *Sci Rep* 2022;12:8784.
53. Yousefi B, LaRiviere MJ, Cohen EA, et al. Combining radiomic phenotypes of non-small cell lung cancer with liquid biopsy data may improve prediction of response to EGFR inhibitors. *Sci Rep* 2021;11:9984.
54. Feng L, Liu Z, Li C, et al. Development and validation of a radiopathomics model to predict pathological complete response to neoadjuvant

chemoradiotherapy in locally advanced rectal cancer: A multicentre observational study. *Lancet Digit Health* 2022;4:e8-e17.
55. Bonazzi VF, Aoude LG, Brosda S, et al. ctDNA as a biomarker of progression in oesophageal adenocarcinoma. *ESMO Open* 2022;7 100452.
56. Hofste LSM, Geerlings MJ, von Rhein D, et al. Circulating tumor DNA-based disease monitoring of patients with locally advanced esophageal cancer. *Cancers (Basel)* 2022;14:4417.
57. Luo H, Wei W, Ye Z, Zheng J, Xu RH. Liquid biopsy of methylation biomarkers in cell-free DNA. *Trends Mol Med* 2021;27:482-500.
58. McClurg DP, Sanghera C, Mukherjee S, Fitzgerald RC, Jones CM. A systematic review of circulating predictive and prognostic biomarkers to aid the personalised use of radiotherapy in the radical treatment of patients with oesophageal cancer. *Radiother Oncol* 2024;195 110224.
59. Booth ME, Smyth EC. Immunotherapy in gastro-oesophageal cancer: Current practice and the future of personalised therapy. *BioDrugs* 2022;36:473-485.
60. Soeratram TT, Creemers A, Meijer SL, et al. Tumor-immune landscape patterns before and after chemoradiation in resectable esophageal adenocarcinomas. *J Pathol* 2022;256:282-296.
61. van Velzen MJM, Derks S, van Grieken NCT, Haj Mohammad N, van Laarhoven HWM. MSI as a predictive factor for treatment outcome of gastroesophageal adenocarcinoma. *Cancer Treat Rev* 2020;86 102024.
62. Cancer Genome Atlas Research N, Analysis Working GroupAsan U, Agency BCC, et al. Integrated genomic characterization of oesophageal carcinoma. *Nature* 2017;541:169-175.
63. Goedegebuure RSA, Harrasser M, de Klerk LK, et al. Pre-treatment tumor-infiltrating T cells influence response to neoadjuvant chemoradiotherapy in esophageal adenocarcinoma. *Oncoimmunology* 2021;10 1954807.
64. Guo L, Du S, Gao S, et al. Delta-radiomics based on dynamic contrast-enhanced MRI predicts pathologic complete response in breast cancer patients treated with neoadjuvant chemotherapy. *Cancers (Basel)* 2022;14:3515.
65. Nardone V, Reginelli A, Grassi R, et al. Delta radiomics: A systematic review. *Radiol Med* 2021;126:1571-1583.
66. Xie D, Xu F, Zhu W, et al. Delta radiomics model for the prediction of progression-free survival time in advanced non-small-cell lung cancer patients after immunotherapy. *Front Oncol* 2022;12 990608.
67. Peeken JC, Asadpour R, Specht K, et al. MRI-based delta-radiomics predicts pathologic complete response in high-grade soft-tissue sarcoma patients treated with neoadjuvant therapy. *Radiother Oncol* 2021;164:73-82.
68. Polverari G, Ceci F, Bertaglia V, et al. ^{18}F-FDG pet parameters and radiomics features analysis in advanced Nsclc treated with immunotherapy as predictors of therapy response and survival. *Cancers (Basel)* 2020;12:1163.
69. Tomaszewski MR, Gillies RJ. The biological meaning of radiomic features. *Radiology* 2021;298:505-516.
70. Fournier L, Costaridou L, Bidaut L, et al. Incorporating radiomics into clinical trials: Expert consensus endorsed by the European Society of Radiology on considerations for data-driven compared to biologically driven quantitative biomarkers. *Eur Radiol* 2021;31:6001-6012.
71. Lambin P, van Stiphout RG, Starmans MH, et al. Predicting outcomes in radiation oncology—multifactorial decision support systems. *Nat Rev Clin Oncol* 2013;10:27-40.